CHIN. PHYS. LETT. Vol. 36, No. 4 (2019) 044301

Acoustic Absorption Characteristics of New Underwater Omnidirectional Absorber *

Cun Wang(王存)[1], Shan-De Li(李善德)[1,2**], Wei-Guang Zheng(郑伟光)[2,3], Qi-Bai Huang(黄其柏)[1,2]

[1]*State Key Laboratory of Digital Manufacturing Equipment and Technology, School of Mechanical Science and Engineering, Huazhong University of Science and Technology, Wuhan 430074*

[2]*Hubei Institute of Specialty Vehicle, Suizhou 441300*

[3]*School of Mechanical and Electrical Engineering, Guilin University of Electronic Technology, Guilin 541004*

(Received 12 December 2018)

We investigate a new underwater omnidirectional absorber with acoustic black hole effect to realize a broadband omnidirectional acoustic wave absorption. Based on multiple scattering theory, a two-dimensional axisymmetric model of underwater omnidirectional absorber comprised of an acoustic gradient refractive index structure and a hollow core is developed, and the mechanisms of omnidirectional absorption and dissipation of acoustic waves are studied. The numerical results indicate that the omnidirectional absorber developed here can achieve the omnidirectional absorption of incident acoustic waves in a broadband frequency and can effectively reduce the backscattering of acoustic waves. It potentially provides a new notion for underwater acoustic coating design.

PACS: 43.20.+g, 43.30.+m DOI: 10.1088/0256-307X/36/4/044301

Gradient refractive index (GRIN) structures have attracted extensive attention and research in the field of optics and acoustics in recent years. It can be used to control the propagation direction of light and acoustic waves, to reduce the scattering of waves, and to realize the bend and focus of waves.[1−11] The optical omnidirectional absorber is a GRIN structure designed to focus incident wave energy to a central absorbing core irrespective of the angle of incidence. Due to the similarity between light wave and acoustic wave equation, the acoustic omnidirectional absorber has become popular recently.[12−18] Climente *et al.*[19] proposed a cylindrical symmetrical omnidirectional absorber consisting of a multilayered shell structure and an absorbing core. The shell can control the direction of acoustic wave propagation to the center, meanwhile the core would dissipate the acoustic energy. The experimental results identify that the structure has effective omnidirectional broadband acoustic absorption in air medium. Elliott *et al.*[20] developed an omnidirectional acoustic absorber based on the acoustic analogy of the electromagnetic metamaterial black hole composed of a hollow cylindrical porous absorbing core and a graded index layer. The numerical results showed that the omnidirectional absorber can obviously improve the efficiency of acoustic absorption and reduce the scattering of acoustic waves. Gu *et al.*[21] designed a two-dimensional omnidirectional absorber consisting of homogeneous anisotropic metamaterials, using matched acoustic impedance to expand the absorption cross section of the absorbing core. The acoustic absorption material has potential applications in the fields of acoustic energy absorption, noise control and so on. Zhang *et al.*[22] proposed an acoustic gradient index system with cylindrical symmetry. The propagation path model of acoustic waves in the gradient structure was established based on the theory of geometric acoustics and a tunable operation mechanism of acoustic waves was realized. Acoustic GRIN structures are mainly studied in air background due to the ease of experimental research in air and due to the fact that the high impedance contrast between solids and air is helpful for the design of metamaterials. The relatively smaller impedance contrast between water and most solids means that a more complicated design scheme is proposed for water. Naify *et al.*[23] designed an acoustic gradient index structure for stealth underwater targets at the US Naval Laboratory. The experimental results suggested that the structure has an appreciable effect of acoustic wave focusing. It has potential application for design of new underwater acoustic coatings.

In this work, we develop a new two-dimensional axisymmetric underwater omnidirectional absorber model with an acoustic GRIN structure and a hollow absorbing core based on multiple scattering theory. The mechanism and effect of the omnidirectional acoustic absorption and dissipation are studied in a broadband frequency, and this study potentially provides a new notion for underwater acoustic coating design.

Figure 1 shows the cross section of a cylindrical omnidirectional absorber, comprising an acoustic GRIN structure and a hollow absorbing core. The acoustic GRIN structure is composed of multilayer cylinders to manipulate the direction of acoustic wave propagation and to provide a smooth transition from the impedance of the background medium to the impedance of absorbing core material. A radially dependent refractive index is achieved by varying the filling rate of each gradient layer, which controls the focus of acoustic waves toward the center.

The refractive index distribution of the acoustic GRIN structure can be expressed by[23]

$$n(r) = \frac{R_1}{r} n_{\mathrm{b}}, \tag{1}$$

*Supported by the National Natural Science Foundation of China under Grant Nos 51575201 and 11204098.

**Corresponding author. Email: lishande@hust.edu.cn

© 2019 Chinese Physical Society and IOP Publishing Ltd

where R_1 denotes the radius of the outermost layer, and n_b refers to the refractive index of the background medium. Figure 2 displays the propagation path of acoustic waves in the GRIN structure. It is refracted at the boundary of each layer when a beam of acoustic waves passes through this medium. The propagation path of acoustic waves in the gradient layer can be controlled by designing the basic parameters of the acoustic GRIN structure.

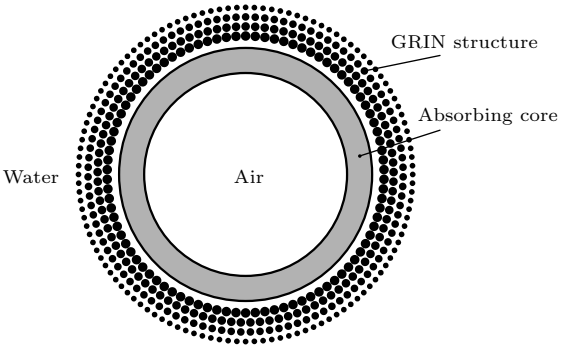

Fig. 1. Cross section of the underwater omnidirectional acoustic absorber.

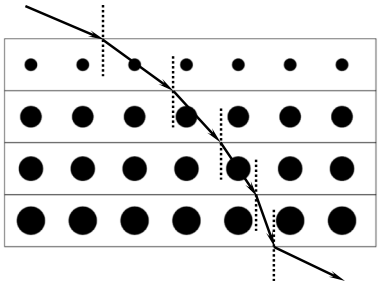

Fig. 2. The propagation path of acoustic waves in the GRIN structure.

The isotropic and homogeneous materials with high dissipation of acoustic energy are used as the absorbing core of the underwater omnidirectional acoustic absorber. Their bulk modulus reads $B' = B(1 + i\gamma)$, where $B = B_\mathrm{b}(r/R_1)^n$ is the coefficient of bulk modulus of the absorbing core, $B_\mathrm{b} = \rho_\mathrm{b} \cdot c_\mathrm{b}^2$ denotes the bulk modulus of the background medium, ρ_b and c_b are density and acoustic velocity of the background medium, respectively, and γ is the loss factor of acoustic waves. Considering the cylindrical layer and a radially varying effective mass density and effective acoustic velocity, the effective acoustic velocity and effective impedance of the acoustic GRIN structure are calculated by the filling rate of the gradient material based the homogeneous theory.[24] To clearly compare the effective parameters between the background medium and the gradient layer, the normalized acoustic velocity is achieved by $c = c_\mathrm{eff}/c_\mathrm{b}$, where c_eff and c_b indicate the effective acoustic velocity of gradient layer and the acoustic velocity of the background medium, respectively. The normalized impedance is achieved by $z = z_\mathrm{eff}/z_\mathrm{b}$, where $z_\mathrm{b} = \rho_\mathrm{b} \cdot c_\mathrm{b}$ denotes the impedance of background medium, and z_eff refers the effective impedance of gradient layer. Figure 3 gives the acoustic velocity and impedance variation rule of normalization inside the acoustic gradient layer.

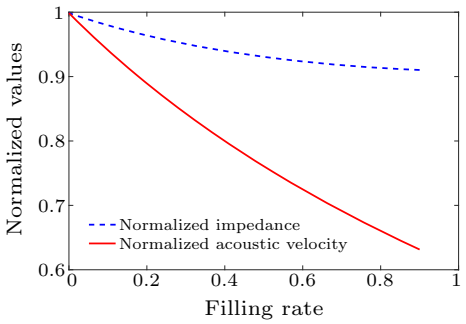

Fig. 3. The acoustic velocity and impedance variation rule of normalization inside the gradient layer.

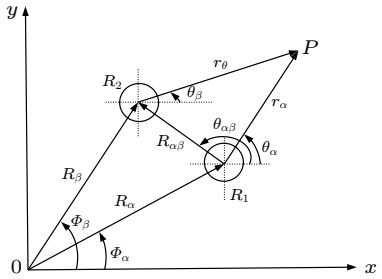

Fig. 4. System of coordinates and definition of variables employed in the expressions of multiple scattering theory.

As shown in Fig. 3, with the increase of filling rate, the effective acoustic velocity of the gradient layer decreases, and the effective impedance of the gradient layer remains closely matched to that of water, so that acoustic waves can enter the gradient layer more effectively. The acoustic gradient layer of the underwater omnidirectional absorber is composed of multilayered cylinders, and the acoustic model can be established using multiple scattering theory.[24] Considering that the model established is a two-dimensional circular axisymmetric acoustic absorption model (see Fig. 1) in this study, N cylinders are located $(R_s,\ \Phi_s)$, $(s = 1, 2, 3, \ldots, N)$ in the background medium in the form of polar coordinates. Figure 4 depicts the system of coordinates and definition of variables employed in the expressions of multiple scattering theory. When acoustic waves are incident on the cylinders, according to the integral definition of Bessel function,[25] the incident acoustic pressure can be achieved by

$$P_\mathrm{b} = \sum_n A_n J_n(k_\mathrm{b} r) e^{in\theta}, \tag{2}$$

where P_b defines the incident acoustic pressure, the wavenumber is $k_\mathrm{b} = w/c_\mathrm{b}$, A_n is the incident coefficient, and J_n is the n-order Bessel function.

The total incident field P_α^inc, which takes into account all the incident waves arriving to the α-cylinder, and the total scattered field P_α^scat in the α-frame[20,26] are

$$P_\alpha^\mathrm{inc} = \sum_n (A_n)_\alpha J_n(k_\mathrm{b} r_\alpha) e^{in\theta_\alpha}, \tag{3}$$

$$P_\alpha^\mathrm{scat} = \sum_m (B_m)_\alpha H_m(k_\mathrm{b} r_\alpha) e^{im\theta_\alpha}, \tag{4}$$

where H_m is the m-order Hankel function of the first kind, $(A_n)_\alpha$ and $(B_m)_\alpha$ are the incident and scattering coefficients of the total incident and scattered fields of the α-cylinder.

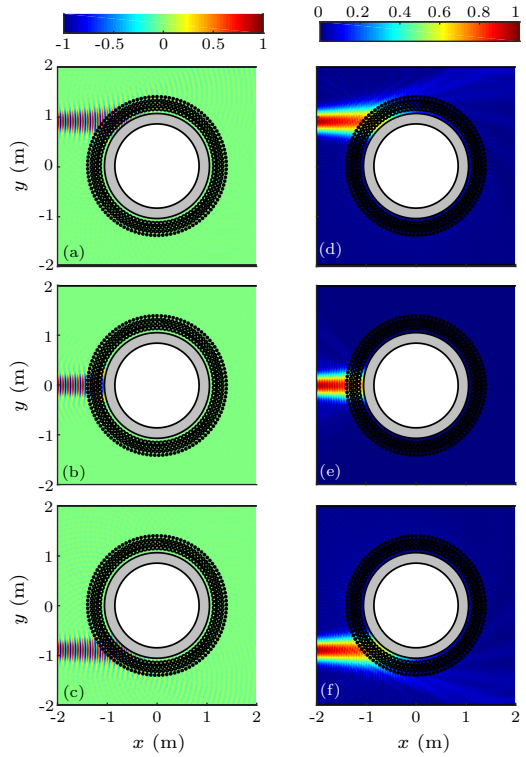

Fig. 5. Pressure fields and intensity fields when a Gaussian beam with frequency 3000 Hz is incident on different regions of the omnidirectional acoustic absorber: (a)–(c) the pressure field, and (d)–(f) the intensity field.

According to Graph's theorem,[25] the total scattered field created by the β-cylinder can be written in the system of coordinates centered at α as

$$P_\beta^{\text{scat}} = \sum_t (B_t)_\beta \sum_n [H_{n-t}(k_\text{b} R_{\alpha\beta}) e^{i(t-n)\Phi_{\alpha\beta}}] \cdot J_n(k_\text{b} r_\alpha) e^{is\theta_\alpha}. \quad (5)$$

The total incident acoustic pressure P_α^{inc} of α-cylinder is equal to the sum of the incident acoustic pressure P_b of initial propagation and the scattered acoustic pressure P_β^{scat} of the other β-cylinder, that is, the total incident acoustic field P_α^{inc} of α-cylinder can be written as

$$P_\alpha^{\text{inc}} = \sum_n (A_n)_\alpha J_n(k_\text{b} r_\alpha) e^{in\theta_\alpha} + \sum_{\alpha\neq\beta} P_\beta^{\text{scat}}. \quad (6)$$

Equations (3), (5) and (6) yield the total scattering coefficient $(B_t)_\beta$, and the total acoustic pressure field of the background medium can be calculated by

$$P(r) = \sum_n A_n J_n(k_\text{b} r) e^{in\theta} + \sum_\alpha \sum_n (B_n)_\alpha H_n(k_\text{b} r_\alpha) e^{in\theta_\alpha}. \quad (7)$$

To verify the effectiveness of the proposed omnidirectional absorber in underwater acoustic absorption, numerical simulations are performed to study the performance of the proposed system. At present, rubber and polyurethane are commonly used underwater acoustic absorbing materials, which are matched with the acoustic impedance of water. These materials can not only maximize the acoustic wave energy into the material, but also have a strong dissipation capacity, which make the acoustic energy attenuation rapid. The outer radius of the proposed structure is $R_1 = 1.44$ m, and the inner radius is $R_2 = 1.06$ m. The layers of the fabricated structure have a common unit cell size of $a = 0.08$ m, the radii of each cylinder in the gradient layer from inside to outside are 0.032 m, 0.028 m, 0.024 m and 0.016 m, respectively. The density of the rubber material is $\rho_\text{a} = 1500\,\text{kg/m}^3$, the acoustic velocity is $c_\text{a} = 1000\,\text{m/s}$, Young's modulus E_b is 0.144 GPa, bulk modulus B_b is 1.2 GPa and Poisson's ratio is $\nu = 0.48$, the density of water is $\rho_\text{b} = 998\,\text{kg/m}^3$, bulk modulus B_a is 2.18 GPa and the acoustic velocity is $c_\text{b} = 1480\,\text{m/s}$. The numerical simulations are implemented using the MATLAB program.

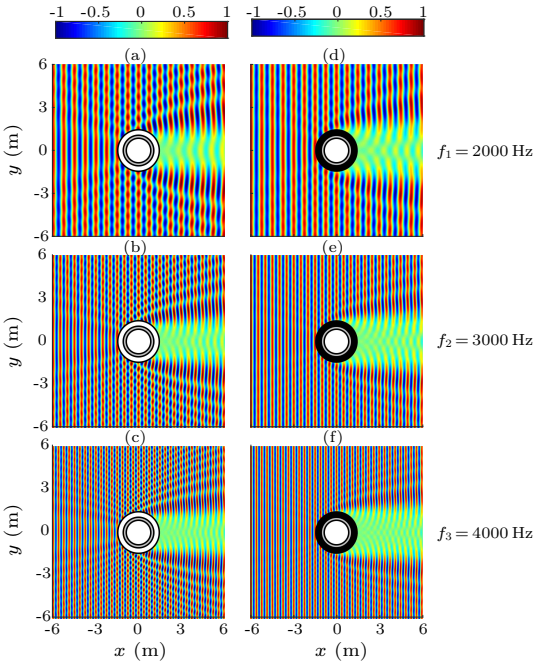

Fig. 6. Pressure field of two kinds of acoustic absorber at different frequencies: (a)–(c) pressure field of acoustic absorber without the gradient layer, (d)–(f) pressure field of acoustic absorber with the gradient layer.

Figure 5 shows the pressure fields and intensity fields when a Gaussian beam is incident on different regions of the omnidirectional acoustic absorber at the frequency 3000 Hz. It is shown that acoustic waves bend toward the center and eventually are absorbed by the core when acoustic waves incident in the upper and lower directions as shown in Figs. 5(a) and 5(e). They enter the absorbing core directly when the acoustic waves enter the gradient layer in the middle direction as shown in Fig. 5(c). It can be clearly observed

from Figs. 5(d)–5(f) that the acoustic energy focuses to the center and dissipates gradually when acoustic waves enter the gradient layer, almost all of the energy is absorbed by the core efficiently and forms a perfect acoustic black hole. The results identify that the underwater omnidirectional absorber developed in this study has effective acoustic wave focusing and acoustic energy dissipation.

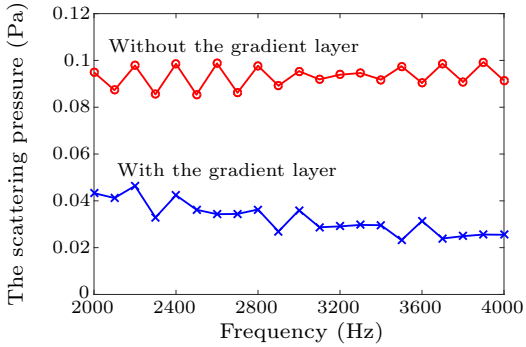

Fig. 7. Comparison of the scattering pressure of two kinds of acoustic absorbers at the reference point in the reverse region.

Furthermore, the mechanism of acoustic wave focusing and dissipation of the omnidirectional absorber is analyzed in the broad frequency. A plane wave is taken as the incident acoustic wave, and the calculated frequency ranges from 2000 Hz to 4000 Hz. Figures 6(a)–6(c) depict the pressure distribution of traditional absorbers without the acoustic gradient layer, and Figs. 6(d)–6(f) show the pressure distribution of underwater omnidirectional absorbers with the acoustic gradient layer. The multiple scattering theoretical calculation includes a reference point located at $(x, y) = (-4, 0)$ m. Figure 7 gives the comparison of the scattering pressure of the reference point in the reverse region between two kinds of absorber models. As shown in Fig. 7, the scattering pressure of omnidirectional absorber with the gradient layer is obviously lower than that of an absorber without the gradient layer for the same frequency. Mainly due to the impedance matching between background medium and the absorber, the scattering pressure decreases when the impedance of water matches well with the impedance of the gradient layer of omnidirectional absorber. It can be seen that the gradient layer has a smooth transition characteristic from the impedance of background medium to the impedance of the absorbed material, which obviously indicates that the acoustic absorption effect of the absorber with the gradient layer is excellent in the broad frequency range, and it is very important for the stealth of underwater targets. Furthermore, the absorption cross section of a bare absorbing core shown in Figs. 6(a)–(c) is significantly enlarged when it is covered by a gradient layer structure, as illustrated in Figs. 6(d)–(f). The reduction of ripples in front of the omnidirectional acoustic absorber with the gradient layer is visible with the gradient layer, which confirms that the front scatters from the structure with the gradient layer are less than those without the gradient layer. It can be seen that the omnidirectional acoustic absorber developed in this study has excellent acoustic absorption in the broadband frequency and effectively reduces the scattering pressure.

In summary, we have proposed a theoretical model of new underwater omnidirectional acoustic absorber based on multiple scattering theory. The research results indicate that the GRIN structure has a smooth transition characteristic from the impedance of the background medium to the impedance of the acoustic absorption material. The new omnidirectional acoustic absorber can effectively control the acoustic wave focusing to the center of the absorber in a board frequency range and dissipate the acoustic energy by the absorber core. It can effectively reduce backscattering and has perfect acoustic black hole effect. In our future studies, piezoelectric and other smart acoustic absorbing materials will be introduced into the absorbing core of the omnidirectional acoustic absorber. The frequency band and effect of the omnidirectional absorber are further improved using its low-frequency acoustic absorbing characteristics, which potentially provide a new notion for underwater acoustic coating designs.

References

[1] Smith D R, Mock J J, Starr A F et al 2005 *Phys. Rev. E* **71** 036609
[2] Centeno E, Cassagne D and Albert J P 2006 *Phys. Rev. B* **73** 235119
[3] Torrent D and Sánchez-Dehesa J 2007 *New J. Phys.* **9** 323
[4] Kildishev A V and Shalaev V M 2008 *Opt. Lett.* **33** 43
[5] Ma C, Escobar A M and Liu Z 2011 *Phys. Rev. B* **84** 195142
[6] Zigoneanu L, Popa B I and Cummer S A 2011 *Phys. Rev. B* **84** 024305
[7] Chang T M, Dupont G, Enoch S et al 2012 *New J. Phys.* **14** 035011
[8] Li Y, Liang B, Tao X et al 2012 *Appl. Phys. Lett.* **101** 233508
[9] Martin T P, Layman C N, Moore K M et al 2012 *Phys. Rev. B* **85** 161103
[10] Xu Z, Qian M L, Cheng Q and Liu X J 2016 *Chin. Phys. Lett.* **33** 114302
[11] Yuan B G, Tian Y, Cheng Y and Liu X J 2016 *Chin. Phys. B* **25** 104301
[12] Li R Q, Zhu X Y, Liang B et al 2011 *Appl. Phys. Lett.* **99** 193507
[13] Hyun J and Wang S 2016 *J. Appl. Phys.* **120** 185103
[14] Zhang H, Liang B, Zou X Y et al 2017 *Appl. Phys. Express* **10** 027201
[15] Chong B M P, Tan L B, Lim K M et al 2017 *Int. J. Appl. Mech.* **9** 1750078
[16] Bobrovnitskii Y I and Tomilina T M 2018 *Acoust. Phys.* **64** 519
[17] Zhou X Q and Yu D Y 2018 *Aerosp. Sci. Technol.* **81** 237
[18] Li X and Ding Q 2018 *J. Vib. Acoust.* **439** 287
[19] Climente A, Torrent D and Dehesa J S 2012 *Appl. Phys. Lett.* **100** 144103
[20] Elliott A S, Venegas R, Groby J P et al 2014 *J. Appl. Phys.* **115** 204902
[21] Gu Z M, Liang B, Li Y et al 2015 *J. Appl. Phys.* **117** 074502
[22] Zhang Z, Li R Q, Liang B et al 2015 *Chin. Phys. B* **24** 024301
[23] Naify C J, Martin T P, Layman C N et al 2014 *Appl. Phys. Lett.* **104** 073505
[24] Torrent D and Dehesa J S 2006 *Phys. Rev. B* **74** 224305
[25] Abramowitz M and Stegun I 1965 *Handbook of Mathematical Functions* (New York: Dover Publications)
[26] Climente A 2015 *PhD Dissertation* (Spain: Polytechnic University of Valencia)